Monte Carlo Study of the Second Virial Coefficient of Star Polymers in a Good Solvent

Kaoru Ohno,*,† Kazuhito Shida,‡ Masayuki Kimura,‡ and Yoshiyuki Kawazoe†

Institute of Materials Research, Tohoku University, Sendai 980-77, Japan, and Japan Advanced Institute of Science and Technology, Asahidai, Tatsunokuchi-machi, Nomi-gun, Ishikawa 920-21, Japan

Received May 31, 1995; Revised Manuscript Received November 28, 1995[⊗]

ABSTRACT: The self- and mutual-avoiding effects of two star polymers in a good solvent are studied by means of a simple Monte Carlo sampling technique on a cubic lattice, using an enrichment algorithm. The total number of configurations is determined as a function of the distance between the two star polymers. The radius of gyration of a single star polymer, the second virial coefficient, the effective interstar potential, and the penetration function are evaluated for 3- to 6-arm star polymers. Considerable deviation from the result of the previous naive first-order ϵ-expansion is observed in the penetration function. We also discuss the value of the penetration function in the infinite-arm limit, according to the cone picture.

1. Introduction

The free energy of a solution of star polymers is of interest to study, because it (or the osmotic pressure) is closely related to the equilibrium conformation of star polymers or micelles in a solvent.[1−5] The microscopic derivation of a reliable form of the free energy of a star polymer solution, however, requires accurate statistical calculations for realistic systems. For example, although the excluded volume effect (EVE) is negligible in a solution of "ideal" stars, it is significant in a solution of "real" stars in a good solvent. In order to describe the global effect of excluded volume,[6] one may consider several physical quantities related to the free energy: the radius of gyration, the second virial coefficient, and so forth. The difference between these quantities in real star systems and in ideal star systems offers a measure of the EVE. Scaling theories are sometimes quite effective and successful. For example, they can explain the osmotic pressure behaving as $c^{9/4}$ in a semidilute solution (c denotes the polymer mass concentration, i.e., weight of polymer per unit volume of solution),[7,8] which cannot be derived using the classical Flory−Huggins theory.[1,2,8] The scaling theory, however, cannot give an explicit form for the free energy as a function of c. Therefore, its combination with other analytical approaches like the renormalization-group approach[9−13] or with other numerical approaches such as Monte Carlo simulation[14−21] is necessary for development of the theory. The osmotic pressure Π of a dilute solution of monodisperse star polymers, which have f arms, each consisting of l segments, is expressed in the dilute limit by a power series in the concentration c as

$$\frac{\Pi}{N_A k_B T} = \frac{c}{M} + A_2 c^2 + A_3 c^3 + \dots \qquad (1.1)$$

where N_A is Avogardro's number and $M = flm$ is the molecular weight of one star polymer (m is the molecular weight of one segment). This series is a virial expansion, and A_i ($i = 2, 3, \dots$) is the ith virial coefficient of the solution. Available experimental information about the virial coefficients is mostly limited to A_2, because of the difficulty of the estimation of A_3 and the higher virial coefficients.[22,23] Historically, the second virial coefficient A_2 of a solution of linear stars has been one of the central problems in the theory of polymer solutions.

In the case of good solvents, the EVE is important for understanding the star polymer conformations. The mean square radius of gyration, $\langle r^2\rangle_g$, is a measure of the intrastar EVE, which behaves as[11,12,24]

$$\langle r^2\rangle_g = \frac{1}{2(N+1)^2}\sum_{i=0}^{N}\sum_{j=0}^{N}\langle(\mathbf{r}_i - \mathbf{r}_j)^2\rangle \simeq c(f) l^{2\nu},$$
$$c(f) \sim f^{1-\nu}, \qquad f \to \infty \qquad (1.2)$$

where ν is the correlation-length exponent for a linear chain;[8] for $d = 3$, $\nu = 0.59$. On the other hand, the second virial coefficient A_2 serves as a measure of the interstar EVE in the dilute solution limit. Let us consider star polymers in a dilute solution and use notations $\mathbf{r}_i$ (or $\mathbf{s}_i$) to denote the end point of the ith segment of the first (or second) star polymer, and $\mathbf{r}_0$ (or $\mathbf{s}_0$) to denote the position of the center of the first (second) star polymer. By means of the two-body interaction $u(\mathbf{r}_i - \mathbf{s}_j)$ between two segments i and j of the first and second star polymers, one can express the second virial coefficient A_2 as

$$A_2 = -\frac{N_A}{2VM^2}\int\int P(\{\mathbf{r}\})P(\{\mathbf{s}\}) \times \{\exp[-\beta\sum_{i=0}^{N}\sum_{j=0}^{N} u(\mathbf{r}_i - \mathbf{s}_j)] - 1\}\prod_{k=0}^{N} d\mathbf{r}_k\, d\mathbf{s}_k \qquad (1.3)$$

where V is the volume of the solution, $\beta = 1/k_B T$, and $P(\{\mathbf{r}\})$ is the one-body distribution function of a star polymer normalized as

$$\int P(\{\mathbf{r}\})\prod_{k=1}^{N} d\mathbf{r}_k = 1 \qquad (1.4)$$

The penetration function Ψ,

† Tohoku University.
‡ Japan Advanced Institute of Science and Technology.
⊗ Abstract published in *Advance ACS Abstracts,* February 15, 1996.

0024-9297/96/2229-2269$12.00/0

$$\Psi = \frac{A_2 M^2}{4\pi^{3/2} N_A \langle r^2 \rangle_g^{3/2}} \tag{1.5}$$

which is a combination of the second virial coefficient and the mean square radius of gyration, is often used both experimentally and theoretically, since it is known to be a universal quantity in the long-chain limit.

In the present paper, we consider a lattice model of a star-polymer solution consisting of just two star polymers and perform a simple Monte Carlo sampling simulation based on an enrichment algorithm.[14−17] We calculate (1) the radius of gyration of single star polymer, (2) the total number of configurations of the two star polymers as a function of f, l, and D, where D is the distance between the centers, (3) the pair distribution function $g(l,D)$ of star polymers in the dilute solution limit, which is related to the interstar potential, and (4) the second virial coefficient and penetration function. We increase l and f stepwise to 80 and 6, respectively, i.e. stars with up to 6 arms of length up to 80 segments. The enrichment algorithm itself allows us to simulate star polymers with relatively large numbers of arms, e.g. 20−32, but here we confine ourselves to a relatively modest number of arms, because the purpose of this paper is to show the feasibility of the evaluation of the second virial coefficient of stars by our method. We made typically 200 000 star polymer configurations on a simple cubic lattice for every value of l and f.

Although the enrichment algorithm reduces computing time significantly, still a very large amount of time is required to simulate the systems with a large number of arms. Since calculations for each star configuration are independent, the algorithm is suitable for application to the new generation of parallel computers. Hence we employed a CM-5 parallel supercomputer at the Japan Advanced Institute of Science and Technology and carried out the two-star-polymer simulations using an optimized and efficient parallel program developed by ourselves. The feasibility and effectiveness of parallel computing using the present enrichment algorithm will be published elsewhere.[26]

The paper is organized as follows: In section 2, we describe how the enrichment algorithm is applied to the star-polymer solution problem and how the second virial coefficient is calculated. Numerical results are presented in section 3, and section 4 contains our conclusions and observations.

2. Enrichment Algorithm

Using an enrichment algorithm[14−17] based on a simple Monte Carlo sampling technique, we generate a large number of samples of two f-arms star polymers at a distance D apart. Each sample has a total of $2f$ arms. In the enrichment algorithm, we generate $2f$ arms each having the same length l (the "lth generation") from a pre-existing sample having $2f$ arms but with the length $l-1$ (the "$(l-1)$th generation"). The number of arms, $2f$, is fixed throughout the computation. On a simple cubic lattice, discarding the sixth direction in which the arm would fold backward on itself, we have five ways of elongating one end of each arm by one bond. At each step of creating the next generation, the self-avoidance condition is tested; unless this condition is fulfilled, the new generated configuration is discarded. Thus, if we want to obtain all possible lth generation realizations from the M_{l-1} distinct realizations at the $(l-1)$th generation, we have to make $5^{2f}M_{l-1}$ trials (5^{2f} trials for each realization of the $(l-1)$th generation) and discard the unphysical realizations which violate the self-avoidance condition. The expected number M_l' of accepted configurations out of the full number of trial configurations $5^{2f}M_{l-1}$ is given by

$$\frac{M_l'}{M_{l-1}} = \frac{N(l,D)}{N(l-1,D)} = \mu^{2f} \tag{2.1}$$

where $\mu = 4.6838$ is the effective coordination number for self-avoiding walks on the simple cubic lattice.[27] However, in order to obtain enough samples, M_l, for our purpose, the full $5^{2f}M_{l-1}$ trials are not necessary. In principle, many less, e.g. mM_{l-1} ($m \ll 5^{2f}$), Monte Carlo trials are enough to iterate the process with almost the same number of samples at every generation; $M_{l-1} \approx M_l \approx M_{l+1} \approx \ldots$. The condition $M_l/M_{l-1} \geq 1$ is satisfied when we choose $m \geq (5/\mu)^{2f} = (1.0675)^{2f}$. For f as large as $f = 6$, a very small value of m (≈ 2.2) results. In practice, it is better to work with somewhat larger values of m for small l. Moreover, it is necessary to increase gradually the number of samples as the arm length l increases, because one has to avoid an unphysical "bias" caused by the iteration. Regardless of the value of m, this enrichment algorithm for star polymers significantly reduces the computational time. In the present study, we fix the directions of all the $2f$ segments at the first generation corresponding to $l = 1$. Since the actual number of trial configurations made is mM_{l-1} instead of $5^{2f}M_{l-1}$, we have

$$\frac{M_l}{M_{l-1}} = \frac{M_l'}{M_{l-1}} \frac{m}{5^{2f}} = m\left(\frac{\mu}{5}\right)^{2f} \tag{2.2}$$

Combining eqs 2.1 and 2.2, we see that the particular value of the ratio M_l/M_{l-1} yields the desired information on the ratio of the subsequent total numbers of configurations:

$$\frac{N(l,D)}{N(l-1,D)} = \frac{5^{2f}M_l}{mM_{l-1}} \tag{2.3}$$

The subsequent total-number ratio can be evaluated straightforwardly from eq 2.3.

The total-number ratio (2.3) is related to the effective value for the configuration-number exponent $\gamma^{\text{eff}}(f)$. The total number of configurations for large l has an asymptotic behavior

$$N(l,D) \sim \begin{cases} l^{2\gamma^{\text{eff}}(f)-2}\mu^{2fl}, & \text{for } D \to \infty \\ l^{\gamma^{\text{eff}}(2f)-1}\mu^{2fl}, & \text{for } D \to 0 \end{cases} \tag{2.4}$$

Thus we have

$$\frac{N(l,D)}{N(l-1,D)} = \begin{cases} \mu^{2f}\left[1 + \dfrac{2\gamma^{\text{eff}}(f)-2}{l} + O\left(\dfrac{1}{l^2}\right)\right], & \text{for } D \to \infty \\ \mu^{2f}\left[1 + \dfrac{\gamma^{\text{eff}}(2f)-1}{l} + O\left(\dfrac{1}{l^2}\right)\right], & \text{for } D \to 0 \end{cases} \tag{2.5}$$

or, by taking its $(1/2f)$th power,

$$\left[\frac{N(l,D)}{N(l-1,D)}\right]^{1/2f} = \begin{cases} \mu\left[1 + \dfrac{\gamma^{\text{eff}}(f) - 1}{fl} + O\left(\dfrac{1}{l^2}\right)\right], & \text{for } D \to \infty \\ \mu\left[1 + \dfrac{\gamma^{\text{eff}}(2f) - 1}{2fl} + O\left(\dfrac{1}{l^2}\right)\right], & \text{for } D \to 0 \end{cases} \tag{2.6}$$

Consequently the configuration-number exponent γ^{eff} is determined by plotting $[N(l,D)/N(l-1,D)]^{1/2f}$ versus $1/l$ for large l.

In a Monte Carlo simulation based on the enrichment algorithm, one can evaluate directly the successive ratios $\{N(l,D)/N(l-D)\}$. If we multiply these successive ratios from $l = 10$ to $l \gg 10$, for example, we have

$$\frac{N(l,D)}{N(9,D)} = \frac{N(l,D)}{N(l-1,D)}\frac{N(l-1,D)}{N(1-2,D)} \cdots \frac{N(11,D)}{N(10,D)}\frac{N(10,D)}{N(9,D)} \tag{2.7}$$

Then, dividing this function by the same function but with $D = \infty$, we obtain the pair distribution function in the dilute limit:

$$g(l,D) = \frac{N(l,D)}{N(l,\infty)} = \frac{N(l,D)}{N(9,D)}\frac{N(9,\infty)}{N(l,\infty)} = \frac{\dfrac{N(l,D)}{N(l-1,D)} \cdots \dfrac{N(10,D)}{N(9,D)}}{\dfrac{N(l,\infty)}{N(l-1,\infty)} \cdots \dfrac{N(10,\infty)}{N(9,\infty)}} \tag{2.8}$$

In deriving the second equality, we used $N(9,D) = N(9,\infty) = N^2(9)$ for sufficiently large D (In fact this relation holds for all D satisfying $D > 18$), where $N(l)$ denotes the total number of configurations of an isolated star polymer.

In the expression of the second virial coefficient A_2, eq 1.3, usually the two-body interaction $u(\mathbf{r}_i - \mathbf{s}_j)$ is approximated by $(\alpha/\beta)\delta(\mathbf{r}_i - \mathbf{s}_j)$ with an EVE parameter α. Furthermore, in a lattice model, all the spatial integrals are replaced by summations over all lattice points, and the exponential is replaced by

$$\exp[-\alpha \sum_{i=0}^{N}\sum_{j=0}^{N} \delta(\mathbf{r}_i - \mathbf{s}_j)] \to \prod_{i=0}^{N}\prod_{j=0}^{N} (1 - \delta_{\mathbf{r}_i,\mathbf{s}_j}) \tag{2.9}$$

We notice that the total number of configurations $N(l,D)$ of two star polymers separated by a distance $D = \mathbf{r}_0 - \mathbf{s}_0$ is expressed as

$$N(l,D) = N(l)^2 \sum_{\{\mathbf{r}\}}\sum_{\{\mathbf{s}\}} P(\{\mathbf{r}\})P(\{\mathbf{s}\})\delta_{\mathbf{r}_0,\mathbf{s}_0+D} \times \prod_{i=0}^{N}\prod_{j=0}^{N} [1 - \delta_{\mathbf{r}_i,\mathbf{s}_j}] \tag{2.10}$$

Substituting (2.10) in (1.3), we find the relation between the second virial coefficient and the pair distribution function in the dilute limit

$$\frac{A_2 M^2}{N_A} = -\frac{1}{2}\int \{g(l,D) - 1\}\, d\mathbf{D} \tag{2.11}$$

Here we used the relation concerning no interference at $D = \infty$, i.e., $N(l)^2 = N(l,\infty)$. The function approaches zero for small D and goes to unity for large D.

Finally, by substituting eq 2.8 into eq 2.11, we can evaluate the second virial coefficient from the subsequent ratios of the total number of configurations.

3. Results

In order to describe the short range behavior of the pair distribution function, one should use star polymers with extremely long arms. However, in the present simulation, the arm length is limited only up to $l = 80$, which is not long enough to represent the behavior expected in the scaling regime correctly. At this point, we have to pay attention to the starting configurations of the star polymers. Since we assume the center to be a lattice point, obviously we have a condition, $f \le 6$, on a simple cubic lattice. In the present study, we only consider configurations, such that the two centers ($\mathbf{r}_0$ and $\mathbf{s}_0$) are on the same row of the simple cubic lattice. Moreover, we fix all the $2f$ directions of the first-generation segments ($l = 1$). Especially, we assume that the first-generation segments have a preference to point in the directions perpendicular to the line connecting the two centers, i.e. perpendicular to $D = \mathbf{r}_0 - \mathbf{s}_0$. The reason for this assumption is as follows: We found that the simulations assuming different directions of the first-generation segments may lead to somewhat different results of the second virial coefficient, when the length l of each arm is not long enough. This difference becomes significant when we compare two extreme preferences of the first-generation segments: (A) a preference to point inward, i.e., $\mathbf{r}_i - \mathbf{r}_0$ (or $\mathbf{s}_j - \mathbf{s}_0$) points to the center $\mathbf{s}_0$ (or $\mathbf{r}_0$) of the other star polymer, and (B) a preference to point outward, i.e., $\mathbf{r}_i - \mathbf{r}_0$ (or $\mathbf{s}_j - \mathbf{s}_0$) points in the direction $D = \mathbf{r}_0 - \mathbf{s}_0$ (or $-D = \mathbf{s}_0 - \mathbf{r}_0$). The two scenarios give different results mainly because of the effective shift of the position of the two centers; the effective center-to-center distance D^{eff} is shorter than D in case A and longer than D in case B. Therefore in order to arrive at the scaling regime as fast as possible with a relatively short arm length, we assume that the first-generation segments point neither to the other center nor to its opposite.

For each star polymer of given f, we evaluated the subsequent ratio $N(l,D)/N(l-1,D)$ of the total number of configurations for $l = 10-80$ and for 21 different distances, $D = 4-80$. Figure 1 shows the plots of $(N_l/N_{l-1})^{1/2f}$ versus $1/l$ for $f = 3-6$. The asymptotic value in the limit $1/l \to 0$ is close to the effective coordination number $\mu = 4.6838$, as it should be, while the slope of the data is related to the estimate of $\gamma^{\text{eff}}(f)$. When the arm length l decreases, the two star polymers do not interfere anymore and behave as two isolated stars; thus all the curves approach the right uppermost line whose slope is equal to $(\gamma^{\text{eff}}(f) - 1)\mu/f$. On the other hand, when the arm length l increases, the two star centers seem to coincide and all the curves in Figure 1 approach the left lowermost line whose slope is equal to $(\gamma^{\text{eff}}(2f) - 1)\mu/2f$. Somewhere in the middle, there is a crossover between these two behaviors. Estimates for the effective configuration-number exponent $\gamma^{\text{eff}}(f)$ have been obtained from the slopes (see Table 1). These values are consistent with previous studies[15,16,18-21] within the estimate error.

In Figure 2 we show the pair distribution function for $f = 6$ and $l = 20-80$ as a function of D. We fit the pair distribution function to the following expression

$$1 - \exp[-(a_1 D)^{a_2}] \tag{3.1}$$

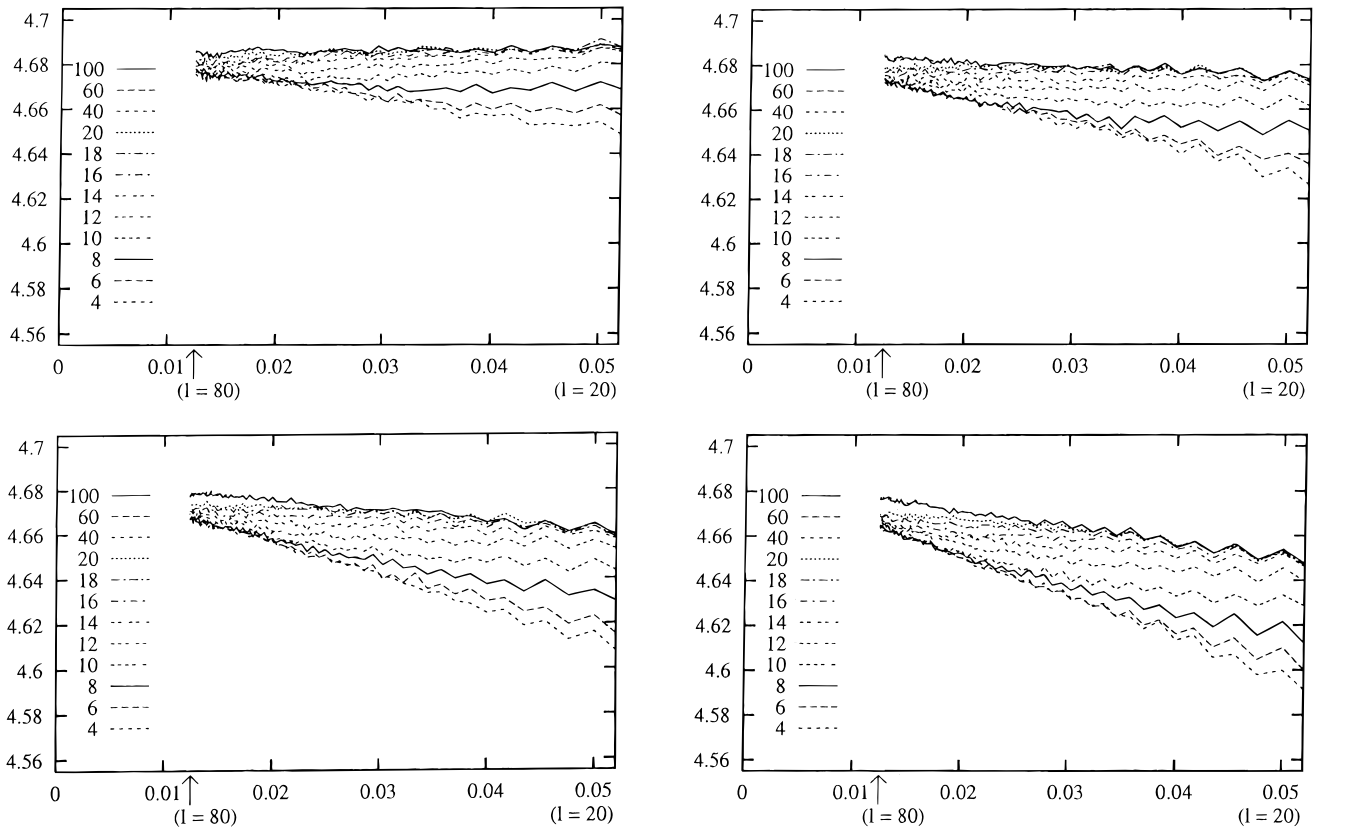

Figure 1. Plot of $[N(l,D)/N(l-1,D)]^{1/2f}$ versus $1/l$ for various values of the center-to-center distance D for two (a) 3-, (b) 4-, (c) 5-, and (d) 6-arm stars. All data approach $\mu = 4.6838$ in the limit $1/l \rightarrow 0$. The slope of the data is related to the effective configuration-number exponent γ^{eff}.

Table 1. Effective Coordination Number Exponent γ^{eff} (Obtained from the Slopes of Data in Figure 1)

topology	f	$\gamma^{\text{eff}}(f)$
two 3-arm stars	3	1.02 ± 0.02
two 4-arm stars	4	0.82 ± 0.04
two 5-arm stars	5	0.48 ± 0.06
two 6-arm stars	6	0.07 ± 0.08

topology	$2f$	$\gamma^{\text{eff}}(2f)$
two 3-arm stars	6	0.11 ± 0.1
two 4-arm stars	8	-0.77 ± 0.2
two 5-arm stars	10	-2.82 ± 0.2
two 6-arm stars	12	-3.41 ± 0.2

which can be integrated analytically to the second virial coefficient using eq 2.11:

$$\frac{A_2 M^2}{N_A} = 2\pi\Gamma\left(1 + \frac{3}{a_2}\right)\frac{1}{3{a_1}^3} \tag{3.2}$$

The calculated second virial coefficient is tabulated in Table 2, together with the radius of gyration of an isolated star polymer defined by eq 1.2 and the penetration function defined by eq 1.5.

Here we comment on the repulsive potential between two star polymers. Witten and Pincus[3] predicted that the interstar repulsive potential $U(l,D)$ is logarithmic in D at short distances. From eq 3.1 we have

$$g(l,D) \propto D^{a_2} \tag{3.3}$$

for $D \sim 0$. Combining eq 3.3 with $g(l,D) \propto \exp[-U(l,D)/k_B T]$, we obtain

$$U(l,D) \sim -a_2 k_B T \log D \tag{3.4}$$

which has the same form as Witten and Pincus's formula. The value a_2 for various l and f determined by our simulation is listed in Table 2 also. Clearly, a_2 has a strong f dependence and we find that it is a monotonic increasing function of f. This behavior is certainly consistent with Witten and Pincus's prediction.

The amplitude $c(f)$ for the radius of gyration is plotted as a function of f on a double logarithmic scale in Figure 3. This behavior should be compared with the second relation of eq 1.2 which was first derived by Daoud and Cotton.[24] The straight line in the figure indicates the theoretical slope. The agreement between the simulation and the theory is quite good. These values are consistent with recent experiments[28] also.

Although the value 0.46 of the penetration function for $f = 4$ is a bit smaller than a previous experiment[29] ($\Psi = 0.53$) and a renormalization-group calculation ($\Psi = 0.53$ up to the first order in ϵ),[10] it agrees well with the recent experiments by Okumoto, Nakamura, and Teramoto[30] ($\Psi = 0.43-0.46$) and Douglas et al.[31] ($\Psi = 0.42-0.47$). When the number of arms f increases, the naive ϵ expansion breaks down because higher powers of f appear in higher order terms of the perturbation expansion.[12] Therefore the ϵ expansion to the first order[7] overestimates the penetration function more and more as f increases. For example, it gives $\Psi = 0.85$ for $f = 6$, $\Psi = 1.28$ for $f = 8$, and even $\Psi = 1.86$ for $f = 10$. In order to obtain reasonable estimates from the renormalization-group analysis, a resummation procedure[12] is required. Unfortunately, there is no such work reported so far concerning the penetration function. An alternative approach is the so-called cone approximation,[12] which is equivalent to Daoud–Cotton's blob picture.[24,25] In the cone picture, the mutual penetration of two stars is prohibited, because each arm is strongly confined to its cone. Therefore, in the limit $f \rightarrow \infty$, a

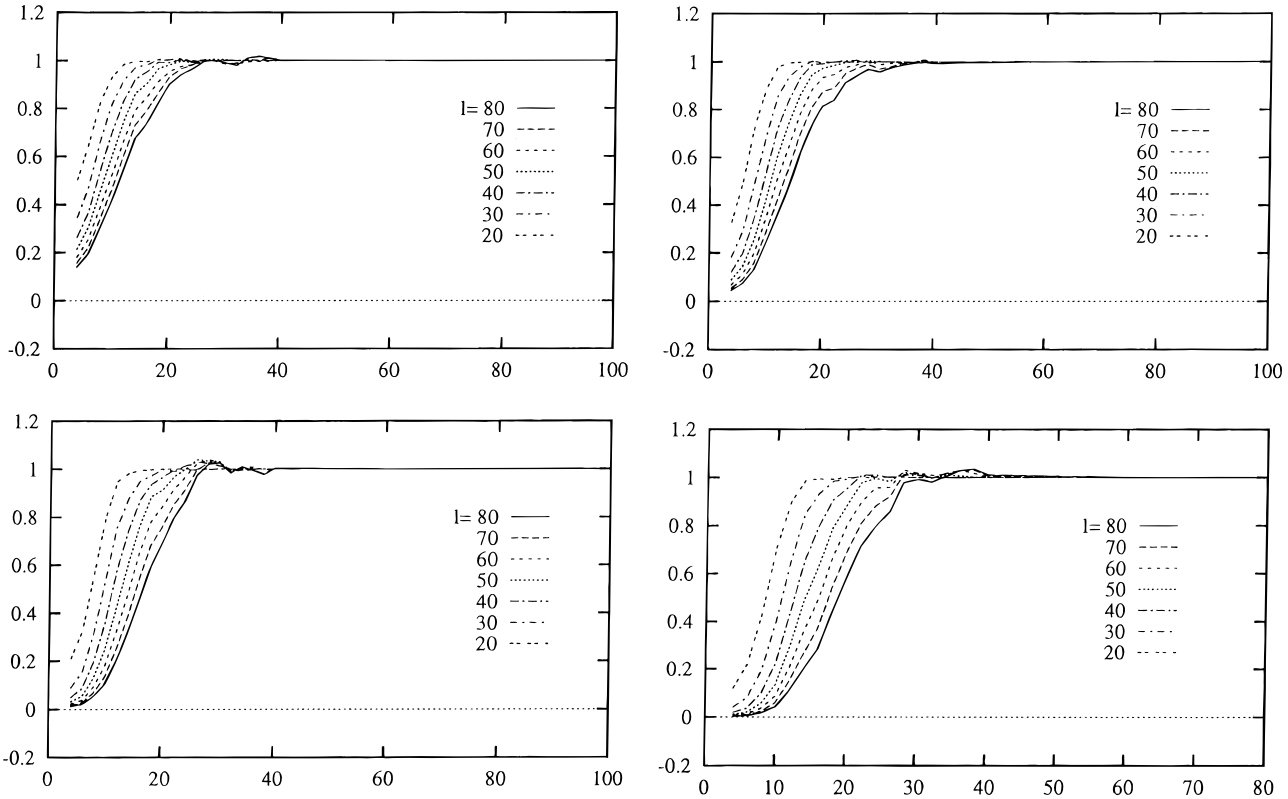

Figure 2. Plot of the pair distribution function $g(l,D)$ versus D for various l values in the dilute limit defined by eq 1.7, for two (a) 3-, (b) 4-, (c) 5-, and (d) 6-arm stars.

Table 2. Resulting Radius of Gyration of an Isolated Star, the Second Virial Coefficient, the Penetration Function, and the Value a_2 in Eq 3.4 for $l = 20-80$ and $f = 3-6$

l	$\langle r^2\rangle_g$	A_2M^2/N_A	Ψ	a_2
		$f = 3$		
20	17.88	678.40	0.40	1.58
30	28.78	1238.57	0.36	1.84
40	40.27	2038.11	0.36	1.95
50	52.37	2948.86	0.35	1.99
60	65.02	4289.77	0.37	1.95
70	78.16	5406.69	0.35	2.01
80	91.38	6735.78	0.35	2.04
		$f = 4$		
20	20.26	857.21	0.42	2.15
30	32.51	1851.68	0.45	2.47
40	45.64	2954.71	0.43	2.65
50	59.17	4189.14	0.41	2.73
60	73.30	5810.62	0.42	2.63
70	88.00	8036.79	0.44	2.49
80	103.08	10622.13	0.46	2.43
		$f = 6$		
20	22.54	1291.97	0.54	2.78
30	35.70	2706.57	0.57	2.95
40	49.61	4310.49	0.55	3.08
50	64.26	6124.36	0.53	3.18
60	79.45	8497.62	0.54	3.12
70	95.13	11287.86	0.55	3.13
80	111.14	13760.61	0.53	3.28
		$f = 6$		
20	23.70	1658.40	0.64	3.35
30	37.73	3305.35	0.64	3.68
40	52.66	5450.91	0.64	3.58
50	68.22	7968.95	0.63	3.69
60	84.36	10761.55	0.62	3.68
70	101.12	14323.36	0.63	3.58
80	118.11	18534.96	0.64	3.50

single star polymer behaves as a hard sphere,[32,33] and the penetration function becomes a constant of order unity. The upper limit of the penetration function for $f = \infty$ stars is estimated in the Appendix; Ψ should approach some value less than 2.13 in the limit $f \to \infty$. Here we notice that the previous experiment by Roovers et al.[28] gives the value 1.1 for the penetration function of both $f = 12$ and $f = 18$ stars.

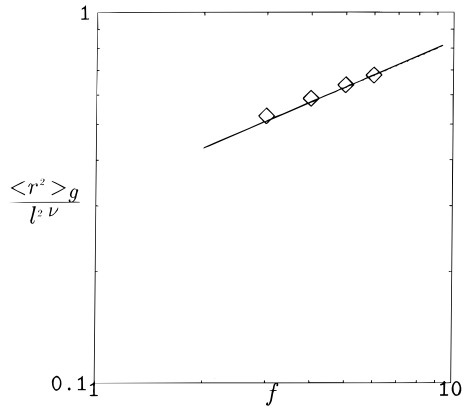

Figure 3. log−log plot of $\langle r^2\rangle_g/l^{2\nu}$ as a function of f for $l = 80$. The straight line indicates the Daoud and Cotton prediction, eq 1.2; $\langle r^2\rangle_g/l^{2\nu} \sim f^{(1-\nu)}$.

4. Concluding Remarks

In this paper, we have successfully applied the enrichment technique of a simple Monte Carlo sampling simulation to study the total number of configurations $N(l,D)$ of two star polymers separated by a distance D. We estimated the radius of gyration of a single star also. From the knowledge of $N(l,D)$, we derived the pair distribution function in the dilute limit, the interstar potential (3.4), and the second virial coefficient. Finally, we estimated the penetration function defined by eq 1.9. The present result for the penetration function was compared with previous experiments, the cone picture,

and the renormalization-group ϵ-expansion studies. Our result significantly deviates from the naive ϵ-expansion result, which indicates the necessity of a resummation procedure.

Acknowledgment. We are grateful to the Information Science Center at JAIST and the Computer Science Group at IMR for their support of computer facilities. K.O. thanks Dr. Y. Nakamura at Osaka University for many useful discussions and for communicating us their result[30] prior to publication. We are also grateful to Professor Marcel Sluiter for his critical reading of our manuscript. This work was partially supported by the Ministry of Education, Science, and Culture (the Grant-in-Aid for Science Research C; Grant No. 05640434).

Appendix

Here we give a short derivation of the penetration in the limit $f \to \infty$ according to the Daoud−Cotton theory.[24] According to this theory, the star polymer is divided into three regions in terms of monomer concentration dependency: core, swollen, and outermost regions. At first, we neglect the outermost region, then the monomer concentration is given as

$$\varrho(r) = \begin{cases} 1.0 & \text{for } r < R_c \text{ (in the core)} \\ R_c/r & \text{for } R_c < r < R \text{ (in swollen region)} \\ 0 & \text{for } R < r \end{cases} \quad \text{(A1)}$$

where R_c is of order $f^{1/2}$. Since the total number of segments is fixed to be $N = fl$, we have

$$\int_0^R \varrho(r) 4\pi r^2 \, dr = -\frac{R_c^3}{6} + \frac{R_c R^2}{2} = fl \quad \text{(A2)}$$

From this we have $R \gg R_c$, if the condition $l \gg f$ is satisfied. Below, we consider such a case only in order to discuss the scaling regime. The radius of gyration is estimated to be

$$\langle r^2 \rangle_g = \frac{\int_0^R \varrho(r) r^2 4\pi r^2 \, dr}{\int_0^R \varrho(r) 4\pi r^2 \, dr} = \frac{-\frac{R_c^4}{5} + R^4}{-\frac{2R_c^2}{3} + 2R^2} \sim \frac{R^2}{2} \quad \text{(A3)}$$

On the other hand, if we assume that two star polymers cannot penetrate to each other and behave as a hard sphere of radius R, the second virial coefficient is given by

$$\frac{A_2 M^2}{N_A} = \frac{2\pi}{3}(2R)^3 = \frac{16\pi}{3}R^3 \quad \text{(A4)}$$

This estimation gives the upperlimit of the second virial coefficient, since a small amount of interpenetration might be allowed even if the number of arms is large. Thus we have the penetration function

$$\Psi = \frac{\frac{16\pi}{3}R^3}{4\pi^{3/2}\langle r^2 \rangle_g^{3/2}} = \frac{\frac{4}{3}\pi}{\left(\frac{1}{2}\pi\right)^{3/2}} = 2.13 \quad \text{(A5)}$$

as the upperlimit value expected at $f \to \infty$. The value given in eq A5 is greater than that of the simple hard spheres, $\Psi = 1.6$. Clearly, this discrepancy is due to the existence of swollen regions in the present estimation.

References and Notes

(1) de Gennes, P. G. In *Solid State Physics*; Liebert, L., Ed.; Academic Press: New York, 1978; Suppl. 14.
(2) Leibler, L.; Orland, H.; Wheeler, J. C. *J. Chem. Phys.* **1983**, *79*, 3550.
(3) Witten, T. A.; Pincus, P. A. *Macromolecules* **1986**, *19*, 2509.
(4) Halperin, A.; Alexander, S. *Macromolecules* **1989**, *22*, 2403.
(5) Merkle, G.; Burchard, W.; Lutz, P.; Freed, K. F.; Gao, J. *Macromolecules* **1993**, *26*, 2736.
(6) Watanabe, H.; Yoshida, H.; Kotaka, T. *Macromolecules* **1988**, *21*, 2175.
(7) des Cloiseaux, J. *J. Phys.* **1975**, *36*, 281.
(8) de Gennes, P. G. *Scaling Concepts in Polymer Physics*; Cornell University Press: Ithaca, NY, 1979.
(9) Miyake, A.; Freed, K. F. *Macromolecules* **1983**, *16*, 1228; **1984**, *17*, 678.
(10) Douglas, J. F.; Freed, K. F. *Macromolecules* **1984**, *17*, 1854.
(11) Ohno, K.; Binder, K. *J. Phys.* **1988**, *49*, 1329.
(12) Ohno, K. *Phys. Rev.* **1989**, *A40*, 1424.
(13) Schäfer, K.; et al. Preprint.
(14) Ohno, K.; Binder, K. *J. Stat. Phys.* **1991**, *64*, 781.
(15) Ohno, K.; Hu, X.; Kawazoe, Y. In *Computer Aided Innovation of New Materials*; Doyama, M., et al., Eds.; Elsevier Scientific Publishers: Amsterdam, 1993; pp 143−146.
(16) Ohno, K. *Macromol. Symp.* **1994**, *81*, 121.
(17) Ohno, K.; Schulz, M.; Binder, K.; Frisch, H. L. *J. Chem. Phys.* **1994**, *101*, 4452.
(18) Lipson, J. E. G.; Whittington, S. G.; Wilkinson, M. K.; Martin, J. L.; Gaunt, D. S. *J. Phys.* **1985**, *A18*, L469.
(19) Wilkinson, M. K.; Gaunt, D. S.; Lipson, J. E. G.; Whittington, S. G. *J. Phys.* **1986**, *A19*, 789,
(20) Batoulis, J.; Kremer, K. *Europhys. Lett.* **1988**, *7*, 683.
(21) Batoulis, J.; Kremer, K. *Macromolecules* **1989**, *22*, 4277.
(22) Fujita, H. *Polymer Solutions*; Elsevier Scientific Publishers: Amsterdam, 1990.
(23) Nakamura, Y.; Norisuye, T.; Teramoto, A. *J. Polym. Sci., Polym. Phys. Ed.* **1991**, *29*, 153.
(24) Daoud, M.; Cotton, J. P. *J. Phys.* **1982**, *43*, 531.
(25) Raphaël, E.; Pincus, P.; Fredrickson, H. *Macromolecules* **1993**, *26*, 1996.
(26) Shida, K.; Ohno, K.; Kimura, M.; Kawazoe, Y. Proceedings of the International Symposium on Parallel and Distributed Supercomputing '95.
(27) Watts, M. G. *J. Phys.* **1975**, *A8*, 61.
(28) Roovers, J.; Hadjichristidis, N.; Fetters, L. *Macromolecules* **1983**, *16*, 214.
(29) Bywater, S. *Adv. Polym. Sci.* **1979**, *30*, 89.
(30) Okumoto, M.; Nakamura, Y.; Teramoto, A. Manuscript in preparation.
(31) Douglas, J. F.; Roovers, J.; Freed, K. F. *Macromolecules* **1990**, *23*, 4168.
(32) Croxton, C. A. *Macromolecules* **1993**, *26*, 3572.
(33) Roovers, J. *Macromolecules* **1994**, *27*, 5359.

MA950742Q